PROCEEDINGS of the
24th International Congress on Acoustics

October 24 to 28, 2022 in Gyeongju, Korea

ABS-0165

Machine-learning-based audio algorithms for cochlear synaptopathy compensation: which speech features are enhanced?

Marjoleen WOUTERS[1]; Fotios DRAKOPOULOS[2]; Sarah VERHULST[3]

[1,2,3] Hearing Technology @ WAVES, Dept. Information Technology, Ghent University, Belgium

ABSTRACT

Auditory models have been used for decades to develop audio signal processing algorithms in hearing aids. Here, we used a biophysically-inspired auditory model, in a differentiable convolutional neural-network (CNN) description (CoNNear), to train different end-to-end machine-learning- (ML) based audio signal processing algorithms that maximally restore cochlear synaptopathy (CS) affected auditory-nerve (AN) responses. Based on the reference normal-hearing (NH) model and a hearing-impaired (HI) model, we used backpropagation to design several ML-based algorithms, using the same CNN encoder-decoder architecture but different loss functions focusing on different aspects of the AN responses. Processing of pure tones and words by the ML-algorithms showed enhanced AN responses to both low- and high-frequency pure tones, and to vowels and consonants in quiet, but responses were usually not restored to the NH-level. The algorithms generally sharpened the onset response to speech and improved the stimulus dynamic range. In an unconstrained operation, the ML-algorithms added more energy to the higher frequencies, degrading speech quality and intelligibility. We will objectively assess the effect of these compensation algorithms on sound quality and speech intelligibility in future clinical experiments.

Keywords: Cochlear Synaptopathy, Machine-Learning, Hearing-Aid Processing

1. INTRODUCTION

Exposure to noise or ototoxic drugs and ageing are common causes of sensorineural hearing loss (SNHL) in humans, and often result in irreversible damage of the outer hair cells (OHCs) or synapses to the auditory nerve (AN), i.e. cochlear synaptopathy (CS) (1, 2, 3). Several studies have suggested that CS results in a loss of the low- (LSR), medium- (MSR) and high-spontaneous rate (HSR) AN fibers (ANFs), in which the LSR and MSR are the first to be lost (2). CS degrades encoding of the temporal envelope in sound, which may contribute to a variety of perceptual abnormalities such as speech-in-noise difficulties and decreased speech intelligibility (2, 4, 5).

However, pure tone audiometric thresholds, related to OHC loss, are not affected in CS, therefore CS is referred to as “hidden hearing loss” (6). Studies on animal models have shown that the loss of ANFs and synapses to the AN, related to cochlear neuropathy and synaptopathy, are the first signs of permanent hearing damage and occur earlier in time than OHC loss (1, 7). Since the audiogram is an insensitive marker for damage to the AN and loss of synapses, patients suffering from CS will experience difficulties understanding speech in challenging situations while their hearing thresholds remain normal. Thus, it is expected that a large group of the noise-exposed or ageing population suffers from CS, which still remains undiagnosed based on their audiogram and will therefore not be treated properly. Non-invasive diagnostic techniques of CS have been recently proposed based on auditory-evoked potentials (AEPs) (8).

The current hearing-aid (HA) algorithms focus on compensating for the elevated audiometric thresholds, but do not specifically compensate for the hearing difficulties related to CS, and therefore offer no treatment to patients who suffer from CS. The non-linear dynamic-range compression strategy of current hearing aids even reduces the amplitude fluctuations of the temporal envelope, what might even worsen the hearing ability in case of CS (9, 10, 11). HA algorithms aiming to compensate for

[1] marjoleen.wouters@ugent.be
[2] fotios.drakopoulos@ugent.be
[3] sarah.verhulst@ugent.be

OHC loss and CS-related hearing impairment hence need to be computationally more complex than standard HA algorithms, in order to be able to grasp the complex non-linear working mechanism of the auditory system.

Auditory models have been used for decades to develop audio signal processing algorithms in HAs. Typically, the difference signal between a normal-hearing (NH) and hearing-impaired (HI) model is used to design such algorithms, but only recently machine-learning (ML) methods have made their entry in this field. Specifically, when adopting differentiable descriptions of biophysical models of hearing-impairment, it is possible to fully backpropagate through the models and design a new type of ML-based audio signal processing that compensates for different aspects of SNHL (12, 13). The objective of this work is to investigate several ML-based HA algorithms able to restore CS, based on a convolutional neural network (CNN) description of a NH and HI auditory model. We will also investigate which sound and speech features are modified when letting several ML algorithms decide the most-optimal solution to compensate for CS.

2. METHODS

2.1 CoNNear Auditory Model

We used a convolutional neural network model of the auditory periphery, CoNNear (14, 15, 16), that was developed starting from a biophysically inspired computational model of the human auditory periphery (17). The CoNNear model provides a fast and differentiable description of the auditory stages (basilar membrane (BM) vibrations, auditory nerve firing, inner-hair-cell (IHC) potential) of the computational model across 201 simulated tonotopic cochlear locations, with center frequencies (CFs) spaced according to the Greenwood place-frequency map of the cochlea (18).

The NH CoNNear model is shown in Figure 1, and simulates the AN response r_F to an auditory input x, sampled at a rate of 20kHz since the CoNNear model operates at a sampling frequency of 20kHz. The CoNNear model consists of three distinct modules: the cochlear stage ($\text{CoNNear}_{\text{cochlea}}$), IHC stage ($\text{CoNNear}_{\text{IHC}}$), and ANF stage. The ANF stage is subdivided in the three different types of ANFs: $\text{CoNNear}_{\text{ANfH}}$, $\text{CoNNear}_{\text{ANfM}}$ and $\text{CoNNear}_{\text{ANfL}}$ for the HSR, MSR and LSR ANFs, respectively. The responses of the three ANF types are combined together to yield the final summed AN response r_F, by using weights H_{NH}, M_{NH} and L_{NH} that correspond to the number of HSR, MSR and LSR fibers in a NH periphery ($H_{NH} = 13$, $M_{NH} = 3$ and $L_{NH} = 3$ as reported in Verhulst et al. (17)). The $\text{CoNNear}_{\text{cochlea}}$, $\text{CoNNear}_{\text{IHC}}$ and $\text{CoNNear}_{\text{ANf}}$ modules comprise encoder-decoder CNN architectures that have the advantage to backpropagate across them, facilitating the development of individualized audio-enhancement methods.

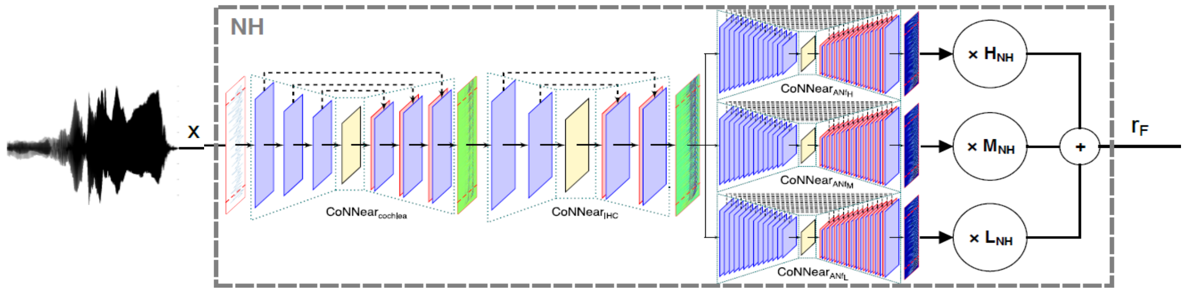

Figure 1 – CoNNear model of the NH auditory periphery (12)

2.2 DNN-Based CS-Compensating HA Algorithms

From the NH CoNNear model, we can obtain a HI CoNNear model by retraining the $\text{CoNNear}_{\text{cochlea}}$ stage via transfer learning to simulate OHC loss (19), and by changing the weights of the different types of ANFs in the $\text{CoNNear}_{\text{ANf}}$ stage to model AN fiber loss, related to CS. The CoNNear HI periphery model can be individualized based on frequency-dependent degrees of OHC loss and CS. The individualized degree of CS and OHC loss of a listener can be obtained from diagnostic measurements using the rectangular amplitude-modulated envelope-following responses (RAM-EFRs) and distortion-product oto-acoustic emissions (DPOAEs), respectively (20, 21).

Consequently, based on the reference NH model and a HI CoNNear model, we can use backpropagation to design ML-based audio signal processing algorithms that optimally compensate for CS (12, 13). The training procedure for a deep-neural-network- (DNN) based HA algorithm has been explained by Drakopoulos et al. (12, 13) and goes as follows: the DNN-HA model processes the input speech x into $\hat{x}$ such that the difference between the NH CoNNear model response r_F and the HI CoNNear model response $\widehat{r_F}$ is minimized. Different CS-compensating HA algorithms can be designed in this way by defining a different loss function (12, 13). These functions can focus on minimizing different aspects of the AN responses (e.g. free training, using more or less cochlear channels, limiting the frequency range, time-domain and frequency representations, also summed across CFs). Thanks to the modular nature of CoNNear, the loss functions can be fine-tuned for each of its distinct modules to optimally compensate for hearing-impairment in each of the modules.

In this work, we trained three DNN-HA models (CS_vow, CS_vow_cons and CS_freq) that to compensate for a hearing-impairment with a CS profile of $H_{HI} = 7$, $M_{HI} = 0$ and $L_{HI} = 0$ ANFs, and no OHC loss. A CNN encoder-decoder architecture was used that comprised 16 layers (8 in the encoder and 8 in the decoder) as described in (12). The three HA models were trained using different loss functions, which are listed in Table 1. A more detailed explanation of the different components of the loss functions that can be used during training is given by Drakopoulos et al. (13). In the CS_vow model, the time-domain AN responses were squared (loss function l_r^2 in (13)) and only AN responses above a certain threshold were minimized (threshold T_r in (13)). The squaring of the time-domain responses was done to emphasize the temporal contrast of the speech envelope modulation to focus the optimization on the enhancement of the most excited regions, since temporal envelope coding is essential for robust speech intelligibility (22, 23). The loss function that focused on only minimizing the AN responses above a specific threshold was applied to further focus on the temporal peaks of the responses. In the CS_vow_cons model, the AN response threshold T_r was applied as well, and an additional loss function was included between the root-mean-square (RMS) difference of the unprocessed and processed signals to ensure that restoration can be achieved without amplification of the stimulus. In the CS_freq model, the loss function l_r^2 was used and a frequency-weighting was applied to emphasize the processing of the low-frequency CFs ($freq.emphasis$ in (13)), so that the high frequencies were processed less than the low. Emphasizing the low CFs in the optimization might achieve better benefits in speech intelligibility since the speech corpus mostly contains energy at low frequencies.

Table 1 – Loss functions used per DNN-HA model

Loss function	CS_vow	CS_vow_cons	CS_freq
Low-frequency CFs emphasized			x
Squared time-domain AN responses	x		x
AN response threshold	x	x	
RMS difference - processed and unprocessed signals		x	

2.3 HA Model Evaluation

The three trained HA models were evaluated on their ability to compensate for the considered CS profile of $H_{HI} = 7$, $M_{HI} = 0$ and $L_{HI} = 0$ ANFs. Post-mortem data from recent temporal-bone studies have shown that NH people have lost more than half of their AN innervations after the age of 50, therefore we chose this CS profile of severe AN fiber loss (24, 25).

Pure tone stimuli and a battery of words in quiet were processed with the three trained DNN-HA models, to evaluate the auditory feature restoration capabilities of the ML algorithms using transfer functions and auditory model simulations. The DNN-HA processed stimuli were given to the HI CoNNear model with the considered CS profile, in order to compare the simulated AN responses of the NH CoNNear model to the responses of the HI CoNNear model, with and without applying the HA processing. This way, we could investigate the difference in responses between the NH and HI models, and see how the HA processing affects the output for the HI case, aiming to restore the AN responses to the NH level. In this work, we present the processing outcomes for several pure tones and the word 'David', extracted from the Flemish Matrix corpus (26). The three pure tones used as input to the DNN-HA models respectively had a frequency of 500Hz, 2kHz and 8kHz with a duration of 404.6ms and an initial silence of 5ms, and were presented at a level of 70 dB SPL relative to the reference pressure $p_0 = 2 \cdot 10^{-5}$Pa, with a sampling frequency of 20kHz. The word 'David' was also presented at 70 dB SPL, with a sampling frequency of 20kHz, and had a duration of 516ms. The DNN-HA models require an input that is a multiple of 256 samples, hence zero-padding was applied at the end of the ‘David’ stimulus.

In order to investigate the transfer-function characteristics of the three HA models, the magnitude spectra of the unprocessed and processed pure tones were visualized. For the word ‘David’ as input stimulus, we analyzed several outputs obtained from the simulated CoNNear AN responses. The first of the three presented outputs is the excitation pattern at the level of the basilar membrane, reflecting the root-mean-square (RMS) over time of the vibration of the BM per CF. The BM excitation patterns shows the vibration amplitude of the BM in function of the CFs along its length, in response to the full input stimulus ‘David’. The second presented output is the excitation pattern at the level of the AN, reflecting the RMS over time of the summed AN response, which is the sum of the simulated firing rates of the HSR, MSR and LSR ANFs, each weighted by their respective number of fibers present (for the HI CoNNear model: $H_{HI} = 7$, $M_{HI} = 0$ and $L_{HI} = 0$; for the NH CoNNear model: $H_{NH} = 13$, $M_{NH} = 3$ and $L_{NH} = 3$), per CF. The third presented output is the wave-1 (W-1) response, which is the sum of the summed AN response across the different frequency channels (CFs), in time, calibrated by a factor in order to match experimentally recorded wave-1 amplitudes.

3. RESULTS

3.1 HA Processing Analysis

We evaluated the auditory feature restoration capabilities of the three trained ML-based HA algorithms, using transfer functions and auditory model simulations as described in the Methods. We present the processing outcomes for several pure tones and a speech stimulus and investigate which auditory features the different HA processing algorithms focused on to compensate for CS.

3.2 Processing of Pure Tones

The magnitude spectra in Figure 2 show the difference in processing between the three HA models CS_vow, CS_vow_cons and CS_freq for pure tones of 500Hz, 2kHz and 8kHz, compared to the unprocessed pure tones that were given as input to the HA models. It can be seen from the plot of the 500Hz pure tone that the processing by the CS_vow model largely enhances the low frequencies and adds energy to the high frequencies in response to a low-frequency stimulus. In the plots of the 2kHz and 8kHz pure tones, the blue curve corresponding to the processing by the CS_vow model is almost zero dB SPL or lower for all frequencies, this HA model hence suppresses high frequencies above the phase locking limit. In the plots of all three pure tones, it can be seen that the CS_vow_cons model adds energy to the high frequencies in the processing to minimize the AN response difference. For the pure tone inputs of both low and high frequencies, this HA model tries to restore the AN response by exciting the CF regions that were not excited by the stimulus before processing. Hence, in this unconstrained operation, the CS_vow_cons model adds more energy to the higher frequencies, which created audible high-frequency tonal components. This effect could be reduced by applying a frequency weighting to the loss functions, which was done in the model CS_freq. It can be seen from the plots that the CS_freq model enhances the low-frequency pure tone of 500Hz, compared to the unprocessed case, and also still enhances the high-frequency input tones of 2kHz but not of 8kHz (due to the frequency weighting). The CS_freq model does this without the addition of high-frequency components. This CS_freq model clearly excites the CF regions closer to the input stimulus frequencies, compared to the CS_vow and CS_vow_cons models.

From these magnitude spectra, we can learn that the combination of loss functions used in the CS_vow model only enhanced the low-frequency pure tones, and failed to enhance the high-frequency tones. The CS_vow_cons and CS_freq models enhanced both low- and high-frequency content, but the lower frequencies in a lesser extent than in the CS_vow model. An additional frequency weighting applied to the loss functions in the CS_freq model avoided the HA model to add too much energy to the high frequencies in the aim to compensate for CS, by focusing the optimization more on the low-frequency CFs. The CS_freq model shows a better energy distribution after processing, this HA model focuses on enhancing the frequencies more close to the input frequency in comparison with CS_vow and CS_vow_cons.

3.3 Processing of a Speech Stimulus

Figure 3 shows the excitation patterns to the input stimulus ‘David’ for the basilar membrane vibration, and Figure 4 shows the excitation pattern of the summed AN response. The different curves on the plots respectively show the simulated response of the NH CoNNear model, the impaired response of the HI model without processing the input stimulus, and the response of the HI model after processing the input stimulus by the three HA models, i.e. the HA-processed responses.

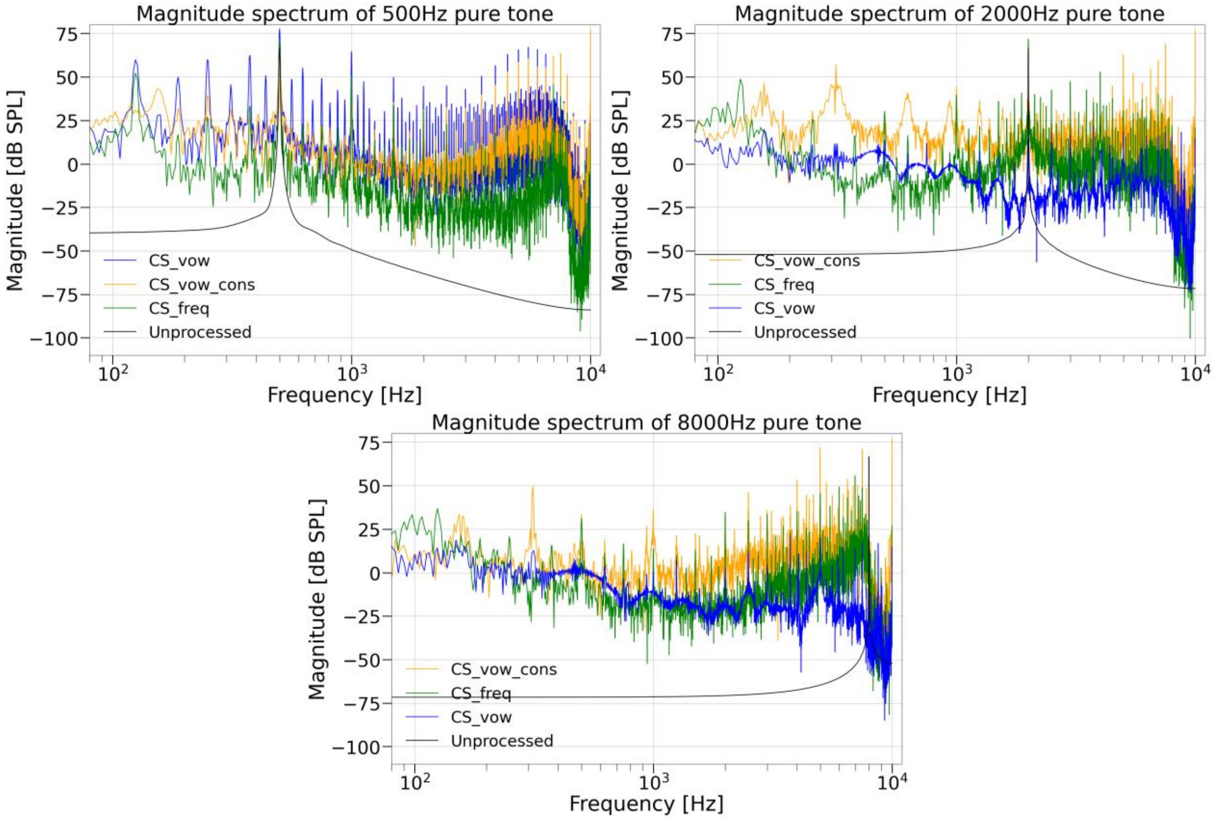

Figure 2 – Magnitude spectra of unprocessed pure tones of 500Hz, 2kHz and 8kHz and their processed versions for the CS_vow, CS_vow_cons and CS_freq HA models

As can be seen from the excitation patterns of the BM vibration in Figure 3, the curves of the NH and unprocessed HI excitation patterns overlap, since the used HI CoNNear model only included CS and no OHC loss. The BM vibration excitation patterns show that the CS_vow model processing amplified all frequencies compared to the unprocessed condition, while this amplification is less pronounced in the CS_vow_cons and CS_freq models. Similar to what we observed in the pure tone magnitude spectra, the CS_vow_cons model added more energy to the high frequencies (above 2kHz), while this effect was reduced in the CS_freq model.

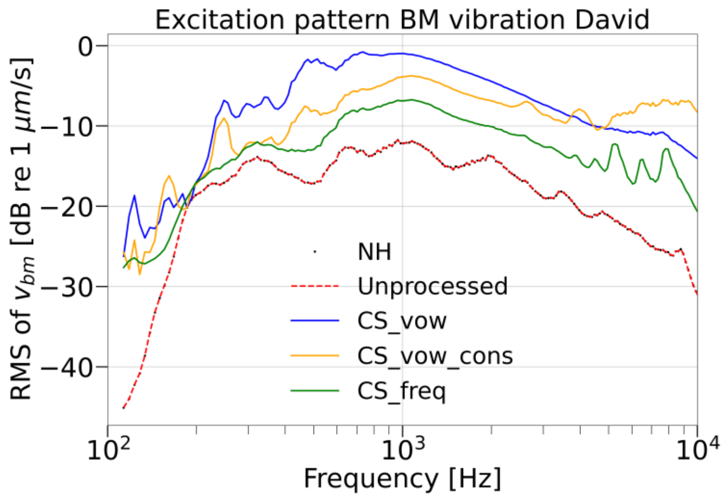

Figure 3 – Excitation patterns showing basilar membrane vibration to the input stimulus ‘David’ for the CS_vow, CS_vow_cons and CS_freq HA models

The excitation patterns of the summed AN responses in Figure 4 already show a clear difference between the NH and HI responses to the unprocessed stimulus. The severe loss of ANFs in our chosen HI CoNNear model significantly decreased the AN responses compared to NH. The summed AN response shows that the CS_vow_cons and CS_freq models slightly increased the firing rate of the ANFs across all frequencies, compared to the unprocessed HI case. We observe again the addition of high-frequency firing in the CS_vow_cons model, creating audible high-frequency tonal components that degraded speech quality and intelligibility. In the CS_vow model, the firing rate is in general attenuated for frequencies below around 2kHz, but the higher frequencies are enhanced, compared to the unprocessed case.

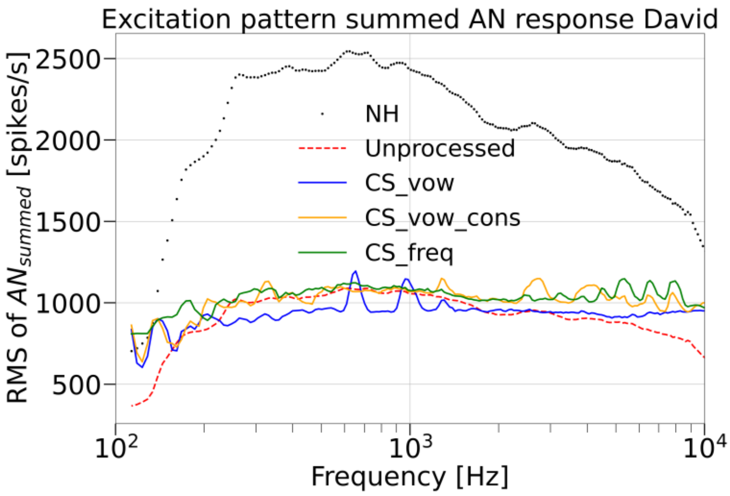

Figure 4 – Excitation patterns showing summed AN response to the input stimulus ‘David’ for the CS_vow, CS_vow_cons and CS_freq HA models

From the plots in Figure 3, it can be observed that all HA models increased the BM vibration over all frequencies, compared to the NH case, but the excitation patterns at the level of the AN in Figure 4 show that the enhancement obtained by the HA processing does not restore the summed AN response to the level of the NH condition at all. We can learn from these Figures that the combination of the loss functions used in the CS_vow model was not able to enhance the firing rate at the level of the AN for low frequencies (below around 2kHz). The CS_vow_cons and CS_freq models better enhanced the excitation at the level of the AN across all CFs, probably due to the restriction of the RMS of the processed output (CS_vow_cons) and the emphasis on the low-frequency content (CS_freq). The frequency weighting in the CS_freq model emphasizing the low frequencies had not much impact on the suppression of the enhancement of the AN firing at high frequencies, compared to CS_vow_cons.

Figure 5 shows the time-domain waveform of the input stimulus ‘David’ and the wave-1 responses to this input stimulus for the three different HA models, compared to the NH and HI unprocessed responses. The occurrence of vowels and consonants is indicated in the plots. From the plots in Figure 5, it can be observed that CS_vow, CS_vow_cons and CS_freq all enhance the wave-1 response to the vowels ‘a’ and ‘i’, compared to the unprocessed HI response. The CS_vow model shows the largest enhancement of vowels, for the vowel ‘i' even to the level of NH, but this HA model shows no response to the consonants ‘d’ and ‘v’, the consonant response is even reduced compared to the HI unprocessed response. The CS_vow_cons model and CS_freq model both show vowel and consonant enhancement, but the wave-1 responses were not restored to the level of NH.

From the plots in Figure 5, we can learn that simultaneous vowel and consonant enhancement could only be obtained when using the combinations of loss functions of the CS_vow_cons and CS_freq models. The algorithms generally sharpened the onset response to speech and improved the stimulus dynamic range. The onset response to both vowels and consonants was especially enhanced in the CS_freq model, by using a loss function of the squared time-domain response that emphasized the temporal contrast of the speech envelope modulation.

4. CONCLUSION

In line with findings of two other studies (12, 13) on ML-based end-to-end CS-compensating algorithms, of which this work is a further application, we showed that such HA algorithms can be designed through backpropagation in a fully automized way, without the need for prior assumptions on the signal processing. The constraints in the loss functions of the trained algorithms cause differences in restored auditory features to compensate for CS. Specifically, the used loss functions influence whether the HA algorithms focus on enhancing low and/or high frequencies, and vowels and/or consonants. Different combinations of loss functions were used to investigate which speech features were enhanced after processing. The CS_vow HA model, trained with a loss function of the squared time-domain responses and that minimized the AN response only above a specific threshold, was only able to enhance the low-frequency pure tones, and the AN response to vowels, not to consonants. The CS_vow_cons model, trained with a loss function on the RMS difference between the processed and unprocessed signal, and that minimized the AN response only above a specific threshold, was able to enhance both low- and high-frequency pure tones and AN responses to both vowels and consonants, but with addition of unwanted high-frequency tones that degraded sound quality. Enhancement of both low- and high-frequency pure tones as well as vowels and consonants was also obtained for the CS_freq model, trained with a loss function that emphasized the low-frequency CFs and that had a loss function of the squared time-domain responses. The latter CS_freq model was the best performing HA model, its loss functions focused most on the low-frequency content, which is most present in the speech corpus, sharpened the onset of the AN response, and emphasized the temporal contrast of the speech envelope modulation, which is beneficial for speech intelligibility. Moreover, the emphasis of the lower frequencies in the CS_freq model reduced the addition of unwanted high frequency components, such that the sound quality was less degraded than in the CS_vow_cons model. However, none of the designed HA models was able to restore the AN response to speech close to the level of NH for the used HI CoNNear model with a severe loss of ANFs. The outcomes of this work suggest that an optimal compensation of such a severe loss of ANFs might not be possible using HA strategies, so the restoration of perceptual-relevant aspects can be a better solution.

In future work, we will objectively assess the effect of these compensation algorithms on sound quality and speech intelligibility in clinical experiments (e.g. Flemish Matrix SRT task). From DPOAEs and RAM-EFRs measurements, we will first assess the patient's CS profile and degree of OHC loss in order to create their individualized HI CoNNear model to use in the backpropagation loop for the design of their individualized DNN-based HA model. Before we can start creating these individualized HA models, we should first optimize the design of the loss functions of the DNN-HA models such that they can optimally compensate for different types of hearing loss. A complete restoration of the severe loss of ANFs that was presented in this work might not be possible, instead we can focus on restoring relevant auditory aspects as much as possible. The CoNNear model can also be expanded with a brainstem processing module in order to more precisely individualize the HI model and restore hearing loss.

ACKNOWLEDGEMENTS

This work was supported by the European Research Council (ERC) under the Horizon 2020 Research and Innovation Programme (grant agreement No 678120 RobSpear).

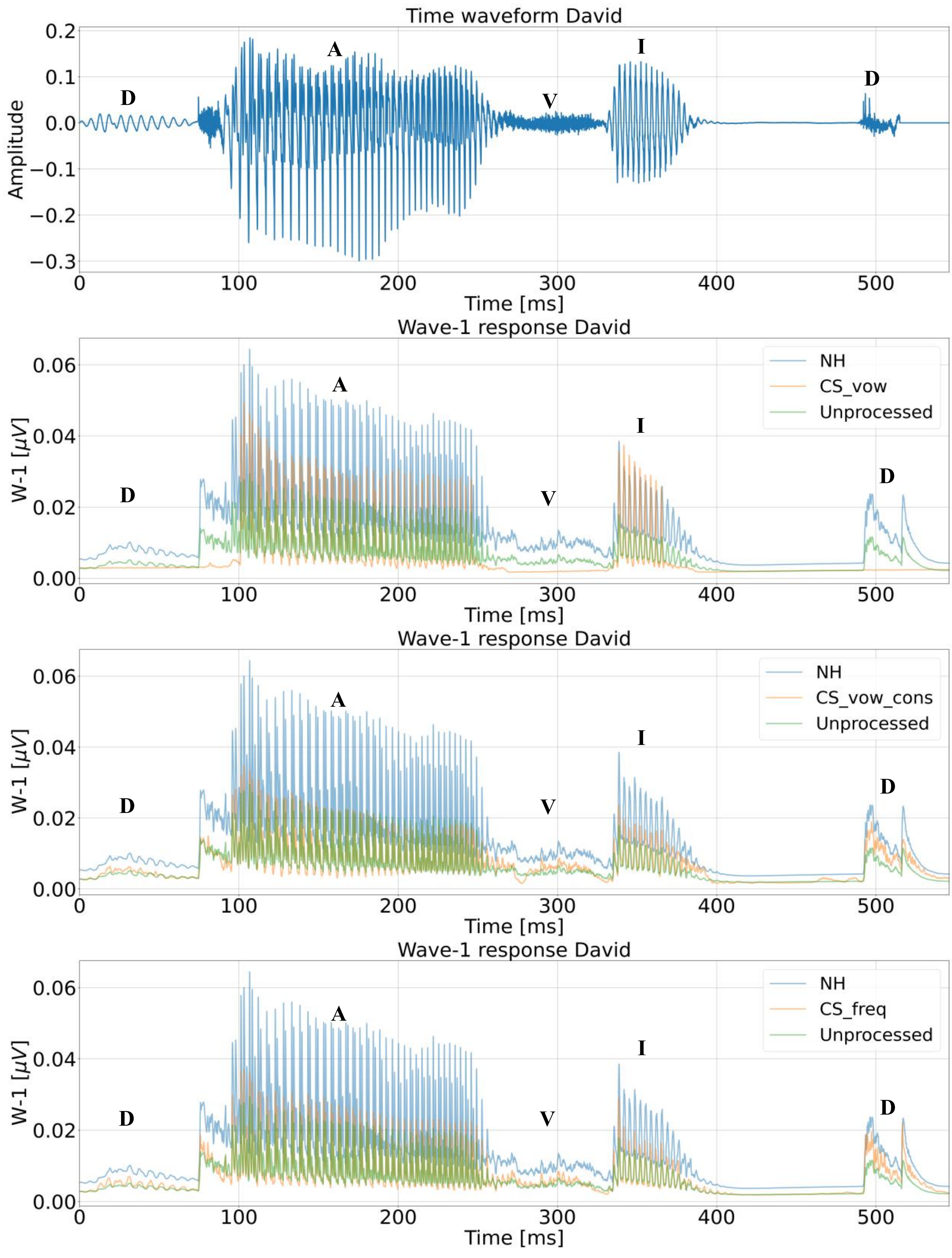

Figure 5 – Time-domain waveform of input stimulus 'David' and the wave-1 responses before and after processing with the CS_vow, CS_vow_cons and CS_freq HA models

REFERENCES

1. Kujawa SG, Liberman MC. Adding insult to injury: Cochlear nerve degeneration after "temporary" noise-induced hearing loss. J Neurosci. 2009;29(45):14077–85.
2. Furman AC, Kujawa SG, Liberman MC. Noise-induced cochlear neuropathy is selective for fibers with

low spontaneous rates. J Neurophysiol. 2013;110(3):577–86.
3. Lobarinas E, Spankovich C, Le Prell CG. Evidence of “hidden hearing loss” following noise exposures that produce robust TTS and ABR wave-I amplitude reductions. Hear Res. 2017;349:155–63.
4. Bharadwaj HM, Verhulst S, Shaheen L, Liberman MC, Shinn-Cunningham BG. Cochlear neuropathy and the coding of supra-threshold sound. Front Syst Neurosci. 2014;8(26).
5. Mepani AM, Verhulst S, Hancock KE, Garrett M, Vasilkov V, Bennett K, et al. Envelope following responses predict speech-in-noise performance in normal-hearing listeners. J Neurophysiol. 2021;125(4):1213–22.
6. Plack CJ, Barker D, Prendergast G. Perceptual consequences of “hidden” hearing loss. Trends Hear. 2014;18:1–11.
7. Sergeyenko Y, Lall K, Liberman MC, Kujawa SG. Age-related cochlear synaptopathy: An early-onset contributor to auditory functional decline. J Neurosci. 2013;33(34):13686–94.
8. Keshishzadeh S, Garrett M, Vasilkov V, Verhulst S. The derived-band envelope following response and its sensitivity to sensorineural hearing deficits. Hear Res. 2020;392:107979.
9. Drullman R, Festen J, Plomp R. Effect of reducing slow temporal modulations on speech reception. J Acoust Soc Am. 1994;95:2670–80.
10. Rance G, McKay C, Grayden D. Perceptual Characterization of Children with Auditory Neuropathy. Ear Hear. 2004;25(1):34–46.
11. Drakopoulos F, Vasilkov V, Osses Vecchi A, Wartenberg T, Verhulst S. Model-based hearing-restoration strategies for cochlear synaptopathy pathologies. bioRxiv. 2022.
12. Drakopoulos F, Verhulst S. A differentiable optimisation framework for the design of individualized DNN-based hearing-aid strategies. In: ICASSP 2022 IEEE International Conference on Acoustics, Speech and Signal Processing (ICASSP). 2022. p. 351–5.
13. Drakopoulos F, Verhulst S. A Neural-Network Framework for the Design of Individualised Hearing-Loss Compensation. Preprint arXiv:2207.07091. 2022.
14. Baby D, Van Den Broucke A, Verhulst S. A convolutional neural-network model of human cochlear mechanics and filter tuning for real-time applications. Nat Mach Intell. 2021;3(2):134–43.
15. Drakopoulos F, Baby D, Verhulst S. A convolutional neural-network framework for modelling auditory sensory cells and synapses. Commun Biol. 2021;4(1).
16. Verhulst S, Baby D, Drakopoulos F, Van Den Broucke A. A neural network model for cochlear mechanics and processing. WO2020249532, 2020.
17. Verhulst S, Altoè A, Vasilkov V. Computational modeling of the human auditory periphery: Auditory-nerve responses, evoked potentials and hearing loss. Hear Res. 2018;360:55–75.
18. Greenwood DD. A cochlear frequency ‐ position function for several species‒29 years later. J Acoust Soc Am. 1990;87:2592-2605.
19. Van Den Broucke A, Baby D, Verhulst S. Hearing-impaired bio-inspired cochlear models for real-time auditory applications. In: Proceedings of the Annual Conference of the International Speech Communication Association, INTERSPEECH. 2020. p. 2842–6.
20. Keshishzadeh S, Verhulst S. Individualized Cochlear Models Based on Distortion Product Otoacoustic Emissions. In: Proceedings of the Annual International Conference of the IEEE Engineering in Medicine and Biology Society, EMBS. 2021. p. 403–7.
21. Keshishzadeh S, Garrett M, Verhulst S. Towards Personalized Auditory Models: Predicting Individual Sensorineural Hearing-Loss Profiles From Recorded Human Auditory Physiology. Trends Hear. 2021;25:1–22.
22. Parthasarathy A, Bartlett EL, Kujawa SG. Age-related Changes in Neural Coding of Envelope Cues: Peripheral Declines and Central Compensation. Neuroscience. 2019;407:21–31.
23. Vasilkov V, Garrett M, Mauermann M, Verhulst S. Enhancing the sensitivity of the envelope-following response for cochlear synaptopathy screening in humans: The role of stimulus envelope. Hear Res. 2021;400:108132.
24. Viana L, O’Malley J, Burgess B, Jones D, Oliveira C, Santos F, et al. Cochlear neuropathy in human presbycusis: confocal analysis of hidden hearing loss in post-mortem tissue. Hear Res. 2015;327:78–88.
25. Wu PZ, Liberman LD, Bennett K, de Gruttola V, O’Malley JT, Liberman MC. Primary Neural Degeneration in the Human Cochlea: Evidence for Hidden Hearing Loss in the Aging Ear. Neuroscience. 2019;407:8–20.
26. Houben R, Koopman J, Luts H, Wagener, KC, van Wieringen A, Verschuure H, Dreschler WA. Development of a Dutch matrix sentence test to assess speech intelligibility in noise. Int J Audiol. 2014;53(10):760–3.

24th INTERNATIONAL CONGRESS ON ACOUSTICS

ICA 2022

October 24(Mon) - 28(Fri), 2022 | Gyeongju, Korea

PROCEEDINGS

Hosted by The Acoustical Society of Korea | ICA